High energy view of the sky with SPI/INTEGRAL Galactic source population component versus diffuse component

L. Bouchet , E. Jourdain and J. P. Roques

Centre d'Etude Spatiale des Rayonnements, CNRS/UPS, B.P. 4346, 31028 Toulouse, France

Abstract.
The INTEGRAL X/γ-ray observatory is a well suited tool to undertake statistical studies of sources emitting at high energy, thanks to the important volume of data accumulated since 2003. We used the SPI/INTEGRAL instrument to build images of the sky at high energy. The study of the emitting sources led to the detection of 197, 96 and 25 persistent sources repectively in the 25-50, 50-100 and 100-300 keV energy bands. We have detected the "diffuse emission" and determined its spatial morphology in longitude and latitude between 20 keV and 8 MeV. Finally, we found that the ratio of diffuse to punctual emission is one-to-tenth below 100 keV. Above 200 keV, the annihilation radiation continuum dominates with a positronium fraction of 97 % and a 511 keV line flux of $\sim 10^{-3}$ photons cm^{-2} s^{-1}. We derived also the galactic central radian log N - log S curve, to help interpreting the measured diffuse to source emission ratio.

Key words. Galaxy: general– gamma rays: observations – surveys – cosmic rays – galaxy : structure – ISM

1. Introduction

The Galaxy Ridge X-rays Emission (hereafter GRXE) hard X-rays (> 20 keV) emission has been previously studied essentially with the CGRO and GRANAT missions (Purcell et al, 1996; Skibo et al., 1997; Kinzer, Purcell & Kurfess, 1999). The main conclusion was that punctual sources strongly contribute to the total emission up to 200 keV, allowing to anticipate that improvement of the future instruments sensibility will allow to resolve an increasing part of what was seen as "diffuse continuum emission". Actually, INTEGRAL results indicate that the GRXE is weak (Lebrun et al., 2004, Terrier et al., 2004, Strong et al., 2005, Bouchet et al., 2005). Krivonos et al. (2007) use the IBIS/INTEGRAL (Ubertini et al., 2003) instrument to obtain an estimate of the GRXE below 200 keV. The good agreement between the estimated longitude and latitude profiles of the GRXE and the galactic distribution of stars obtained from infared observations along with its measured spectrum led to conclusion that sources population of magnetic white dwarfs, polar caps and intermediate polar caps provide a dominant contribution to the Galactic X-ray emission between 20 and 60 keV. In this paper, we measured directly the shape of the "diffuse" continuum emission, by performing an imaging analysis of the sky with SPI/INTEGRAL. We thus present an inventory of the hard X-ray emitters, as well as a measurement of the spatial morphology of the unresolved emission between 25 keV and 8 MeV.

Send offprint requests to: L. Bouchet ; *bouchet@cesr.fr*

2. Instrument and observations

The spectrometer SPI (Vedrenne et al., 2003) onboard ESA's INTEGRAL observatory was launched on 2002, October 17. Its in-flight performance can be found in Roques et al. (2003). Imaging capabilities are obtained through the association of a coded mask with a γ camera that consists of an array of 19 actively cooled high-resolution germanium (Ge) detectors operating between 20 keV and 8 MeV.
We analysed data from 2003 March to 2006 March 30 for a total of 377 revolutions covering the entire sky. Each INTEGRAL orbital revolution lasts 3 $\sim$ days and consists of several exposures (typically, 30-40 minutes pointings dithering around the target). Due to the small number of detectors, imaging relies on these observations in dithering mode (Jensen et al., 2003) ; the pointing direction varying by steps of 2° within a 5×5 square or a 7-point hexagonal pattern. Data polluted by solar flares and radiation belts entry are excluded from the analysis, which results in $\sim$ 25700 exposures for a total observation time of 51×10^6 seconds of effective observing time.

3. Mapping the sky

To map both sources and diffuse emissions at the same time, we have developed an "hybrid" reconstruction algorithm to produce very sensitive maps, in which the sources emissions are extracted by model-fitting while the diffuse/extendedone is imaged simultaneously.

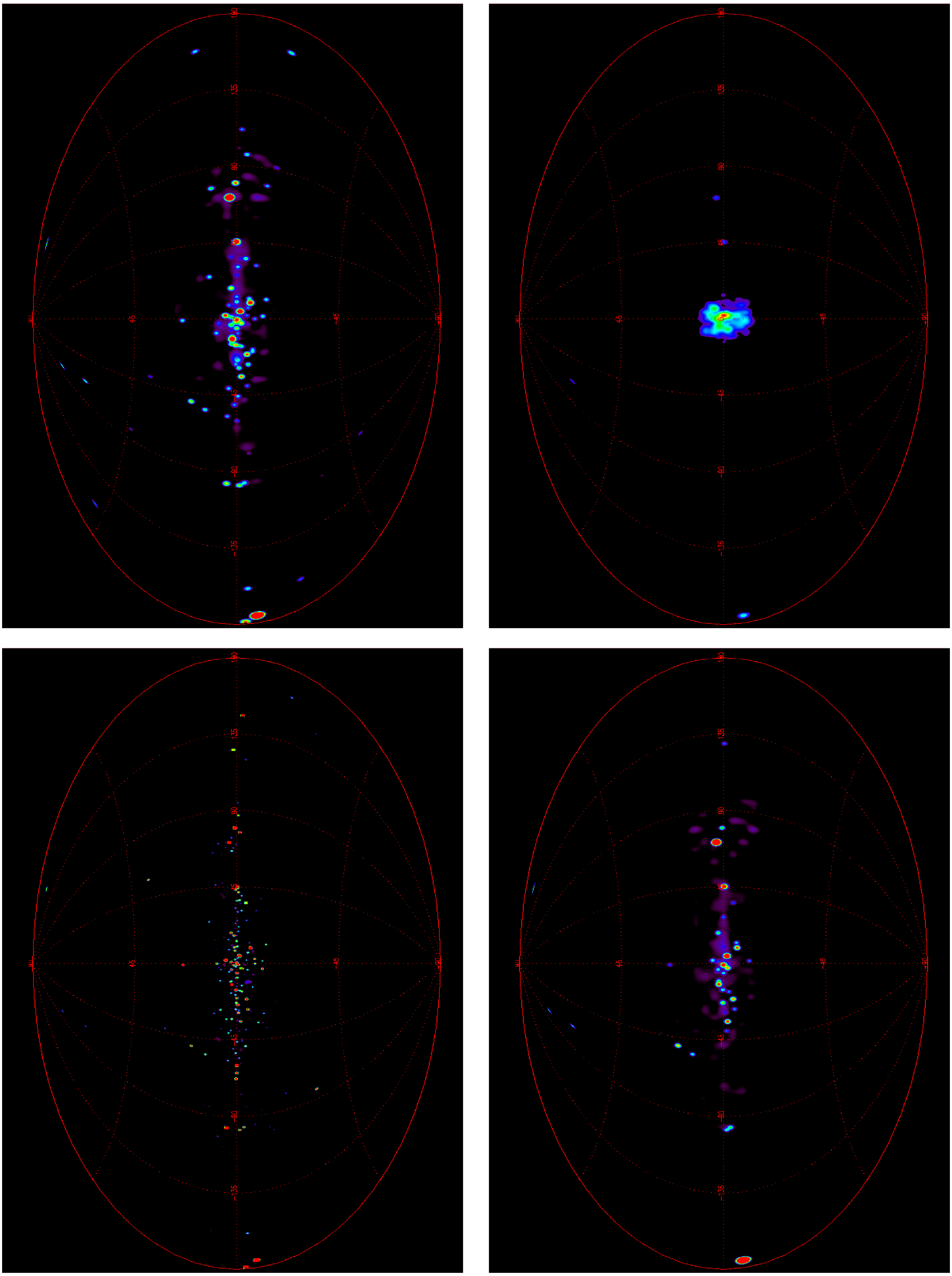

Fig. 1. Sky-maps in the 25-50 keV (bottom-left), 50-100 keV (top-left), 100-300 keV (bottom-right) and 506-516 keV (top-right) energy bands. The images are scaled logarithmically with a rainbow color map (the scale of colors ranges from black (weak), to red (strong)). The scale is saturated to reveal the weakest sources. There is some systematic due to strong variable sources such as Cyg X-1 combined with the finite precision of SPI response, especially in the 25-50 keV band. We take into account this systematic using a higher threshold in those region.

Briefly, the image pixel size depends on whether we search for sources or for extended (diffuse) emission : small size pixels provided non-reported excesses potentially associated with sources while large pixels are better to search for flux in the underlying low signal-to-noise ratio ascribed to "diffuse emission".

The developed algorithm can also naturally handle sources and background variabilities, which constitute the main difficulties in images reconstruction. Images are obtained iteratively using both our hybrid algorithm and the SPIROS software delivered in the INTEGRAL OSA (Offline Science Analysis) package as descrided in Bouchet et al. (2005). Briefly, in first step, we have the algorithm with small pixel to complete the catalogue. Then, once the catalogue built, we rerun the algorithm with large pixel size. The resulting catalogues contain 197, 96 and 25 sources detected above 4σ respectively in the 25-50 keV, 50-100 keV and 100-300 keV. The catalogue between 300 and 600 keV contains 10 sources ($> 4\,\sigma$), while above 600 keV only Crab Nebula, Cyg X-1 and GRS1915+105 are detected. Figure 1 shows sky images at different energies and illustrates how the sky is dominated by the sources emission at low- energy and then becomes dominated above 300 keV by the "diffuse emission", mainly from the annihilation radiation spectrum.

4. Diffuse spatial morphology

Spatial modeling of the annihilation radiation spectrum (line + positronium continuum) has been made in details using SPI/INTEGRAL (Knodlseder et al., 2005, Weidenspointner et al., 2006). This component is well ajusted with an axisymmetric Gaussian profile of $\sim$ 8° FWHM. Here we concentrate on the GRXE spatial distribution. The measured profiles are shown in fig 2 and 3 compared to CO and NIR Dirbe 4.9 μ maps (http://lambda.gsfc.nasa.gov) corrected from reddening. Both models represent adequatly SPI longitude profiles. Latitude profiles are better described by the Dirbe map especially below $\sim$ 100 keV. But, the 25-50 keV one shows some enlargement compared to these maps. Nevertheless, it is expected, based on the current understanding of the GRXE morphology, that the best tracer is the NIR surface brightness (Revnivtsev et al., 2006, Krivonos et al., 2007) at energies lower than $\sim$ 200 keV.

4.1. The galactic central radian - diffuse emission vs. punctual emission

Fig. 4 shows the different components of the Galaxy emission derived assuming that the GRXE emission morphology is described by the Dirbe 4.9 μ below 200 keV and CO map above. The annihilation radiation morphology has been fixed to an axisymmetric Gaussian shape centered at (l,b)=(0°,0°) with FWHM of 8°. The derived diffuse continuum spectrum can be modeled with a power law of index $\sim$ 1.7-1.8 above 50 keV, but required an additional component below 50 keV. The component below 50 keV can be explained in terms of individual sources, a populations of accreting magnetic white dwarfs being expected to provide a dominant contribution to the Galactic X-ray emission in this energy band (Krivonos et al., 2007).

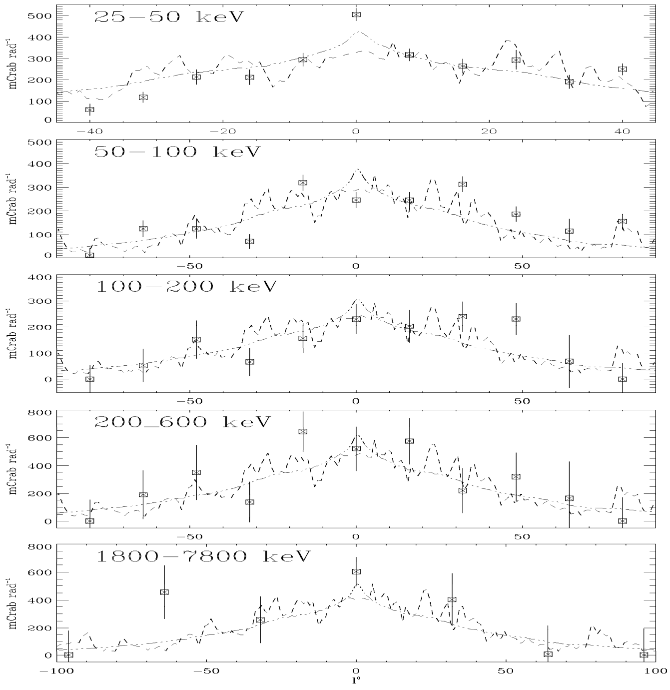

Fig. 2. Longitude profiles in different energy band for $|b| \leq 4°$. Dotted and dashed line correspond respectively to the CO and NIR 4.9 μ map.

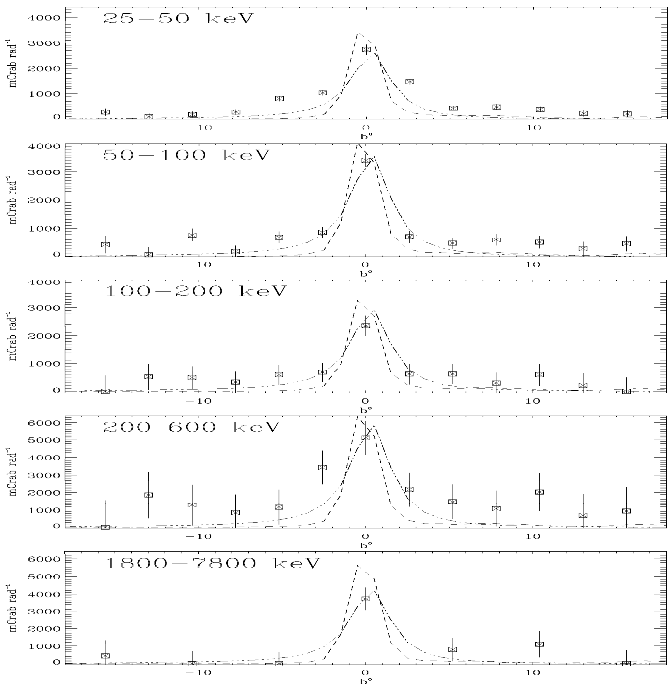

Fig. 3. Latitude profiles in different energy band for $|l| \leq 28°$. Dotted and dashed line correspond respectively to the CO and NIR 4.9 μ map.

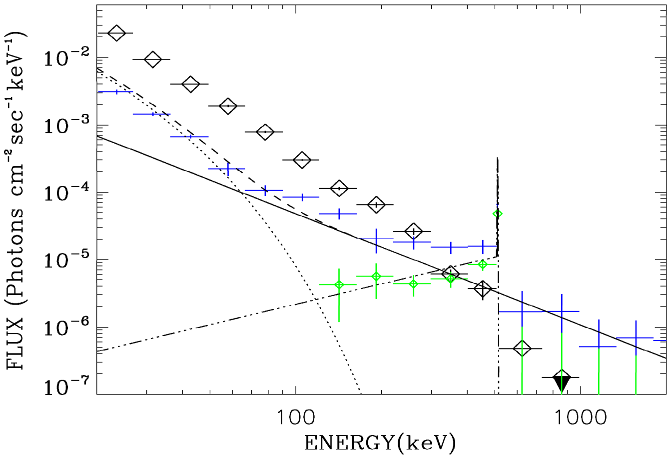

Fig. 4. Spectra of the different emission components, total sources (diamonds), annihilation spectrum (light crosses with diamond), total diffuse (crosses). Thelines are the emission models obtained from previous measurements (Bouchet et al., 2005).

5. Central radian sources intensity distribution - log N-log F curves

In order to give more reliable results on the ratio of sources to total emission and consequently on diffuse emission, we have to estimate how much emission is coming from soources is missed by SPI due to the sensitivity limit, we have invsetigate the source intensity distribution function. We have thus derived log N-log F curves for the central region ($|\ l\ | \leq 30°$, $|\ b\ | \leq 15°$) in several energy bands. These distributions were corrected from the non-uniform region exposure : we have simulated a set of sources with a given power law index distribution, with the pointing directions and durations having the statistical properties of the original dataset. We then reconstructed the fluxes (and calculate standard deviation of each sources) to build a log N-log F curve for sources above 4σ threshold. The ratios between the reconstructed and injected flux distribution curves are used to correct the measured curves. (Fig 5). We change the power law index of the sources distribution until the fit data power law index, after correction, matches the observed one. The final power law indexes found are fully compatible with those obtained by Dean et al. (2005) and Bazzano et al. (2006) with IBIS/INTEGRAL. Actually, the SPI limiting fluxes are 2.5 (5σ), 4.2 (4σ) and 3.4 (4σ) mCrab respectively in the 25-50, 50-100 and 100-300 keV bands. The source to total emission ratio measured are 91, 85 and 58 % respectively in the 25-50, 50-100 and 100-300 keV bands Assuming that the total exposure time will double at the term of the mission, we will be able to measure source to total emission ratios in the following ranges 92-100, 87-94, 61-66 % and for a survey with a limiting flux of 1 mcrab, 93-100, 90-100, 69-92 %. The lower values assumed that possible new sources are currently mixed with background flux, while the upper values assumed that they are currently considered as "diffuse" the total flux being kept constant. For the most optimistic scenario, we should be able to measured an actually constraining value for the diffuse emission below 100 keV at the end of INTEGRAL mission.

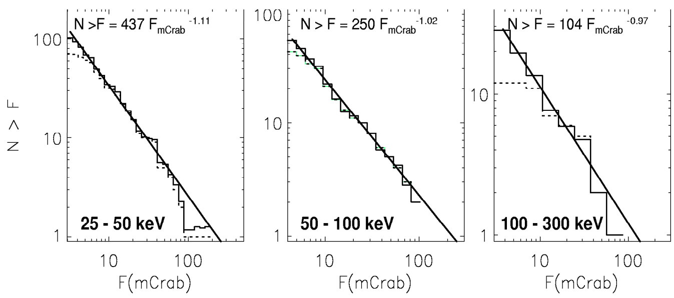

Fig. 5. log N - log F curves for the region $|l| \leq 30°$ and $|b| \leq 15°$. Dashed line are the measured curve before correction (solid line). Thick lines are the fitted power law model, whose parameters are given in insert.

6. Conclusions

It has been suggested that the most part of the GRXE emission between 20 and 60 keV can be interpreted in terms of a population of accreting magnetic white dwarfs (Krivonos et al., 2007). The same authors that their data between 60 and 200 keV are compatible with no GRXE at these energies. We have detected a weak emission in this energy band, on the other hand extrapolation toward fainter sources of the sources distribution using the log N - log F curves, shows that if the GRXE emission is really non-diffuse, we should be able to measured it since the INTEGRAL mission lifetime is extended (so far confirmed until 2010). However, spectrum of the GRXE needs further investigation to assess biases introduced by the assumed spatial distribution (NIR or CO), this topicwill be the subjet future research. On the other hand we clearly detected the annihilation radiation spectrum as well as a diffuse broad emission between 200 keV and 8 MeV, with in particular the annihilation radiation contribution.

References

Bazzano A. et al., 2006, 649, L9-12
Bouchet et al., 2005, ApJ, 635, 1115
Dean A.J. et al, 2005, A&A, 443, 485
Jensen P.L. et al., 2003, A&A, 411, L7
Kinzer R.L. et al. 1999, ApJ, 515, 215
Knödlseder J. et al., 2005,A&A, 441, 513
Krivonos, R. et al., 2007, A&A, 463, 957
Lebrun F. et al., 2004, Nature, 428, 293
Purcell W.R. et al., 1996, A&AS, 120, 389
Revnivtsev, M. et al.,2006, A&A, 452, 169
Roques J.P. et al, 2003, A&A, 411, L91
Skibo, J. G. et al., 1997, ApJletters, 483, L95
Strong, A. W. et al., 2005, A&A ,444,495
Ubertini P. et al, 2003, A&A, 411, L131
Terrier, R., et al., 2004, Proc. 5th INTEGRAL Workshop, ESA SP-552, p513; astro-ph/0405207
Vedrenne G. et al, 2003, A&A, 411, L63
Weidenspointner G. et al, 2006, A&A, 450, 1013